ACTA RADIOLOGICA

OFFICIAL ORGAN OF THE RADIOLOGICAL SOCIETIES OF DENMARK, FINLAND, NORWAY AND SWEDEN

Vol. 15 Fasc. 2 | THERAPY PHYSICS BIOLOGY | 1976 April

TISSUE HETEROGENEITY IN THE ANTERIOR CHEST WALL AND ITS INFLUENCE ON RADIATION THERAPY OF THE INTERNAL MAMMARY LYMPH NODES

B. LINDSKOUG and A. HULTBORN

Investigation of tissue heterogeneities

This report is a continuation and revision of a previous work concerning distribution of the absorbed dose in post-operative irradiation of regional lymph nodes in mammary carcinoma (RAGNHULT et coll. 1972). On the basis of experimental measurements it was demonstrated that a considerable distortion of the absorbed dose distribution occurred when lymph glands along the internal thoracic vessels were irradiated with high-energy electrons. The absorption of electrons will depend on the stopping power, which is approximately proportional to the electron density of the absorbing medium, i.e. the most important of the parameters influencing the interaction of electrons with matter. In the previous report it was realised that a survey of the electron densities of the various tissue materials in the anterior chest wall was needed. A method for determination of electron density of fresh autopsy specimens without loosing clinical aspects was developed and tested with materials of well known composition. Further measurements have now been per-

From the Departments of Radiation Physics (Director: Assoc. Prof. H. Sköldborn) and Radiation Therapy (Director: Prof. G. Notter), University of Gothenburg, S-413 45 Gothenburg, Sweden.

Submitted for publication 13 February 1975.

7 – 765846

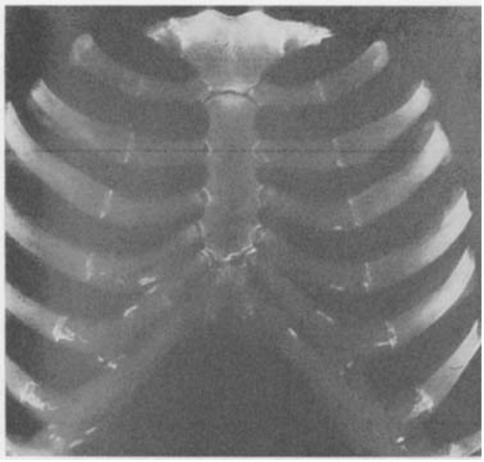

Fig. 1

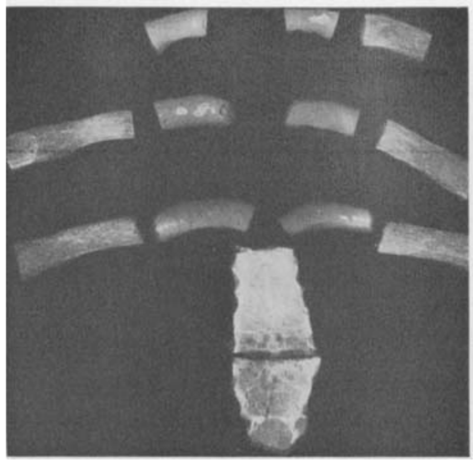

Fig. 2

Fig. 1. Specimen No. 2 of the anterior chest wall.

Fig. 2. Specimen No. 4 of sternum, rib bone and costal cartilage.

formed and complemented by a more comprehensive review of the pertinent literature. Determinations were made on specimens from 8 autopsies.

Preparation. Ages and sexes of the patients appear in Table 1, together with the time-lag between death and autopsy. Within a few hours post-mortem the bodies were transferred to cold storage and maintained at 4°C until specimens were removed, which in all cases occurred within four days.

Fig. 1 demonstrates a specimen of cartilage, bone and soft tissue from the anterior wall of the thorax—corresponding to a parasternal electron field. In order to obtain results which could be considered valid and applicable in radiation therapy it was essential to avoid influencing the material mechanically and chemically, as far as

Table 1

Particularities of the specimens used

Specimen number	Age	Sex	Delay between death and autopsy (days)
1	63	M	0.5
2	49	F	4
3	54	F	1
4	61	F	1
5	76	F	3
6	66	M	3
7	81	F	3
8	61	F	1

Table 2

Results of density measurements. Number of specimens measured within brackets (SD = standard deviation)

Cartilage, bone

Specimen number	Costal cartilage g cm^{-3}	Costal cartilage SD	Rib bone g cm^{-3}	Rib bone SD	Sternum g cm^{-3}	Sternum SD
1	(5) 1.137	0.013	(3) 1.298	0.042	(1) 1.266	
2	(6) 1.138	0.006	(6) 1.277	0.018	(1) 1.123	
3	(6) 1.126	0.005	(6) 1.208	0.023	(1) 1.096	
4	(6) 1.116	0.009	(5) 1.142	0.028	(2) 1.065	0.012
5	(6) 1.126	0.008	(6) 1.203	0.024	(2) 1.093	0.004
6	(6) 1.119	0.003	(6) 1.170	0.026	(4) 1.050	0.003
Over all mean value	(35) 1.127	0.011	(32) 1.211	0.057	(11) 1.091	0.063

Soft tissues

Specimen number	Muscle tissue g cm^{-3}	Muscle tissue SD	Muscle tissue with fat g cm^{-3}	Muscle tissue with fat SD	Fatty tissue g cm^{-3}	Fatty tissue SD
7	(2) 1.056	0.003			(2) 0.940	0.005
8			(3) 1.034	0.006	(5) 0.918	0.003
Over all mean value	(2) 1.056	0.003	(3) 1.034	0.006	(7) 0.924	0.011

Remark:

Specimen No. 7. Tissue from m. pectoralis. Visible courses of connective and fatty tissue were removed.
Fatty tissue from subcutis, anterolaterally on the thorax and from the abdominal wall.

Specimen No. 8. Tissue from m. pectoralis and m. serratus anterior with many courses of connective and fatty tissue.
Subcutaneous fatty tissue from the mammary region.

possible. Soft tissue was removed from the surfaces of sternum, ribs and costal cartilage by dissection (Fig. 2).

Determination of density. The density was determined by weighing the specimens in air and in distilled water by means of a precision balance. The temperature of the water was checked repeatedly and the corresponding density was used in the calculations. The measurements were made at room temperature, which varied between 20 and 24°C. The specimens were suspended in the balance by a thread. Material with a density less than 1 was provided with a sinker. The results of density determination are included in Table 2.

Extraction of fatty tissue and creation of air cavities in the spongy parts of sternum and ribs had to be avoided as far as possible (cf. DEBOIS et coll. 1969). Especially close to the cut surfaces in sternum and ribs, the spaces between the trabeculae have a tendency to trap air bubbles or fluid. In order to estimate the error under those conditions two series of measurements were performed on specimen 3. The maximum deviation occurred, as expected, for ribs, and amounted to 0.012 g cm^{-3}.

Immediately after the density determination the specimens were closely packed into plastic beakers for the determination of electron content.

Determination of electron content. Since it was a prerequisite that the results should be clinically applicable, narrow-beam geometry, which requires fresh autopsy specimens in the form of plane discs, could not be used. An apparatus designed for determination of the mineral content of lumbar vertebrae by measurement of transmission (ROOS et coll. 1970) proved to be well suited for the purpose. The radiation source consisted of ^{137}Cs which decays under emission of photons with an energy of 662 keV. At this photon energy the interaction with matter is strongly dominated by the Compton effect. As the average Compton collision cross-section per electron depends only on the photon energy, the probability of an interaction between a photon and the specimen will depend only on the electron content of the material. Thus, by determining the attenuation of the photon beam for a specimen of unknown composition and comparing the result with the attenuation obtained for a well known reference material, the electron content of the specimen could be determined.

The design of the measuring equipment is illustrated in Fig. 3. During measurements the preparations were stored in plastic beakers (diameter 25 mm, height 50 mm).

Theoretical considerations. The following notations were used:

I, number of counts per minute
$\left(\frac{\mu}{\varrho}\right)$, mass-attenuation coefficient (cm^2 g^{-1})
${}_e\sigma$, Compton attenuation cross-section per electron (cm^2)
ϱx, dimension of the specimen (g cm^{-2})
m, mass of the specimen (g)
A_{eff}, effective area of the specimen in the plane of measurement (cm^2)
η, electron content (g^{-1}).

The common exponential expression for the attenuation of a photon beam is only valid with narrow-beam geometry

$$I = I_0 \exp\left[-\left(\frac{\mu}{\varrho}\right)\varrho x\right] \tag{1}$$

The mass-attenuation coefficient (μ/ϱ) may also be written as

$$\frac{\mu}{\varrho} = \eta\, {}_e\sigma \tag{2}$$

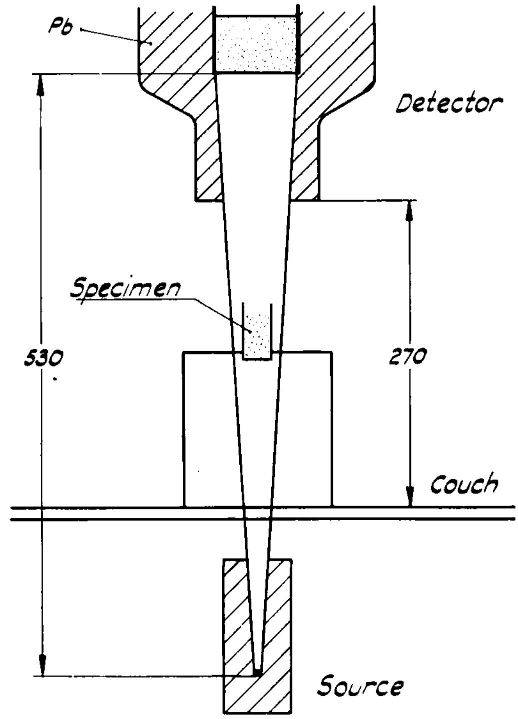

Fig. 3. Principle for transmission measurements. The radiation source ^{137}Cs. The specimen is placed in a beaker. Dimensions in mm.

If a specimen in the beaker can be assigned an effective cross-sectional area, A_{eff}, for which the exponential relationship (1) is approximately valid and introducing the parameter,

$$F = \frac{_e\sigma}{A_{eff}} \tag{3}$$

is obtained

$$I = I_0 \exp\left[-Fm\eta\right] \tag{4}$$

F will be dependent upon geometry and mass of the specimen and if different volumes were used considerable errors might occur.

Before and after each preparation measurement the reference material (distilled water) was introduced in the radiation beam and the counting rate recorded. The following notations were introduced:

I_r and I_{or}, number of counts per minute with reference material and empty beaker respectively,

m_n and m_r, mass of specimen and reference material, respectively, in grams,

η_n and η_r, number of electrons per gram for specimen and reference material, respectively.

Table 3

Results of electron content determination of test material. Comparison with calculated values. Calculated electron content included

Material	Electron content $g^{-1} \times 10^{-24}$ Calculated	Measured	Density $g\ cm^{-3}$	Electron density $cm^{-3} \times 10^{-24}$
Perspex $C_5H_8O_2$				
Homogeneous rod*	0.324	0.325	1.186	0.385
Loosely packed rods**		0.320		0.380
Tightly packed rods**		0.326		0.387
Crushed perspex		0.325		0.385
Tricalciumphosphate				
Powder (pro anal.)				
$Ca_5(PO_4)_3(OH)$	0.300	0.305	2.528	0.771
Oleic acid				
Liquid $C_{17}H_{33}COOH$	0.337	0.331	0.887	0.294

* Dimension 25 mm × 20 mm.
** Dimension 5 mm × 10 mm and 10 mm × 10 mm.

If F had the same value for both specimen and reference material,

$$\frac{\eta_n m_n}{\eta_r m_r} = \frac{\ln(I_n/I_{on})}{\ln(I_r/I_{or})} \tag{5}$$

The masses of the specimen and the reference material were determined by weighing before and after the transmission measurements. The electron content (η_r) for the reference material was calculated to be 3.34 10^{23} g^{-1} and the electron content of the specimen (η_n) was computed from the formula (6),

$$\eta_n = 3.34 \cdot 10^{23} \frac{m_r}{m_n} \frac{\ln(I_n/I_{on})}{\ln(I_r/I_{or})} \tag{6}$$

Finally, the product of the densities of the specimens and the corresponding electron content gave the quantity sought, i.e. the electron densities for the specimens.

Experimental tests of method. To check the method a number of test materials of known compositions but different configurations were used. Table 3 summarizes the results and also gives the calculated values, for comparison. It was essential for several reasons to keep the counting rate approximately equal for both reference material and specimen: (1) the statistical error should be of the same magnitude; (2) the ratio of the logarithms in equation (6) should be close to 1, thus, giving a minimum error of edge effects; (3) the scatter contribution to the counting rate should be of the same order of magnitude for both reference material and specimen.

Table 4

Results of electron content determination of specimen

Cartilage, bone

Specimen number	Costal cartilage $g^{-1} \times 10^{-24}$	Rib bone $g^{-1} \times 10^{-24}$	Sternum $g^{-1} \times 10^{-24}$
5	0.321	0.309	0.324
6	0.309	0.294	0.317
Mean value:	0.315	0.302	0.320

Soft tissues

Specimen number	Muscle tissue $g^{-1} \times 10^{-24}$	Muscle tissue with fat $g^{-1} \times 10^{-24}$	Fatty tissue $g^{-1} \times 10^{-24}$
7	0.334		0.334
8		0.330	0.330
Mean value:	0.334	0.330	0.332

Specimens 7 and 8; see remark Table 2.

The most important errors probably originate from variations in the scatter contribution for the different materials. Thus, the shape of the specimen and the filling of the beaker will influence on the magnitude of the error. This point was indicated by the test measurements. In Table 3 results with different-shaped perspex were included. Cylindrical rods of various dimensions gave a deviation of 1.2 per cent with loose packing but only 0.6 per cent with tight packing. Small pieces of crushed perspex gave the same result as for a homogeneous rod, deviating only 0.3 per cent from the calculated value. Powder with very high density (2.5 g cm^{-3}) and a liquid with very low density (0.89 g cm^{-3}) gave a deviation of +1.7 per cent and −1.8 per cent, respectively. Obviously, a close filling with a homogeneous material of a density of the same magnitude as the reference material will give the best results.

Examination of specimens. Immediately after preparation and determination of density the specimens were submitted to transmission measurements.

1) The balance was adjusted to zero with the empty beaker. The beaker was then filled with the specimen as closely packed as possible. The weight of the specimen was recorded.
2) The counting rate was measured with an empty beaker in the beam.
3) The empty beaker was filled with distilled water and the weight was determined.
4) The counting rate was measured with the distilled water in the beam.
5) The counting rate was measured with the specimen in the beam.
6) The weight of the distilled water was recorded.
7) The weight of the specimen was recorded.
8) Measurement number 2 was repeated.

Table 5

Results of electron density determination in material from the anterior chest wall

Material	Density g cm^{-3}	Electron content $g^{-1} \times 10^{24}$	Electron density $cm^{-3} \times 10^{24}$	Relative electron density
Rib bone	1.211	0.302	0.366	1.099
Costal cartilage	1.127	0.315	0.355	1.066
Sternum	1.091	0.320	0.349	1.048
Muscle tissue*	1.056	0.334	0.353	1.060
Muscle tissue with fat	1.034	0.330	0.341	1.024
Fatty tissue	0.924	0.332	0.307	0.922
Water	0.997	0.334	0.333	1.000

* Connective and fatty tissue macroscopically removed.

Measurement number 2 had to be repeated because of temperature drifting of the instruments. Due to evaporation the specimens had to be weighed both before and after the transmission measurements. The counting rate with empty beaker was of the order of 300 000 counts per minute. For every measurement five values were registered, each integrated over one minute. The mean value of the five readings were used for the calculations, which were performed using a desk calculator.

The sternum caused special problems during preparation, since it is composed of highly vascular spongy bone with a marrow containing blood cells and fat cells enclosed in a thin compact bone. The problems were overcome in the following way. By means of a circular metal tube with a sharp edge a number of circular plates were punched out of the sternum in dorsoventral direction. The tube was of the same internal diameter (25 mm) as the beaker in which he specimens were placed during measurement. From the tube the plates were gently pushed directly into the beaker. With this method liquids inside the sternum were preserved and the risk of changing the composition was exceedingly small.

Results

The results of the density determinations in cartilage and bone are given in Table 2. As expected, the dispersion was greatest for spongy bones.

In spite of the calcific deposits (Figs 1, 2) the costal cartilage varied only little in density. The standard deviation is about 1 per cent. The over all mean density of sternum was found to be 1.09 g cm^{-3} with a standard deviation of 0.06. Similar measurements on human sternum were made by BOONE et coll. (1969), who reported a value of 1.15 g cm^{-3}.

The soft tissue densities are in good agreement with the results reported by TRÜBESTEIN (1960). He reports for pectoralis major 1.050 g cm^{-3} at 36°C. In fatty tissue

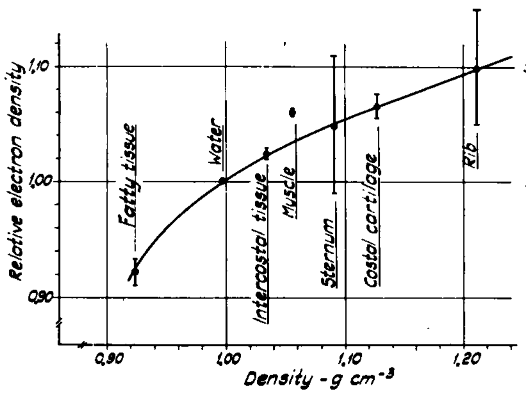

Fig. 4

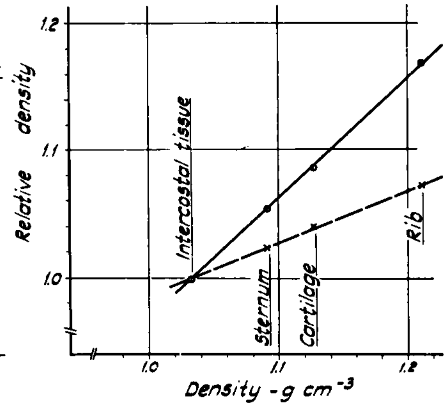

Fig. 5

Fig. 4. Relative electron density of tissues from the anterior chest wall.

Fig. 5. Relative density (——) and relative electron density (---) for sternum, costal cartilage and rib bone, normalized to intercostal soft tissue.

he found a considerable variation in density depending on the water content. With 7.7 per cent H_2O he reports 0.924 and with 42.0 per cent H_2O 1.017 g cm^{-3}. The water content was not considered in the present investigation.

The results of the determinations of electron content appear in Table 4. It is apparent that the variation in electron content in the anterior chest wall might amount to about ± 5 per cent.

In Table 5 the over-all mean values of density and electron content and the electron densities computed from the determined values in the different types of specimens are given and in the last column the ratios to the electron density for water.

The relative electron densities for the various tissues in the anterior chest wall were plotted against density (Fig. 4). As the water content of fatty tissues will influence the density, the value 1.017 g cm^{-3} found by TRÜBESTEIN for fat containing 42 per cent H_2O, must also be considered. In that case the relative electron density will be 1.020, a value lying very close to the value found for intercostal tissue.

Discussion

Several approximate methods have been proposed for calculating the influence of a heterogeneity on the distribution of absorbed dose in radiation therapy with electrons (DUTREIX 1966, POHLIT 1969, BOONE et coll. 1969, DAHLER et coll. 1969). However, no simple method seems to exist for those cases in which elastic scattering is the dominant effect. This is the case for heterogeneities having small cross-sectional areas and for regions where there is a great difference in electron density between the heterogeneity and the surrounding medium (KARJALAINEN et coll. 1968). BRENNER et coll. (1969) have demonstrated that scattering effects have a considerable

Table 6

Calculated and measured electron content in various tissue compounds

Tissue	Electron content $g^{-1} \times 10^{-23}$
Muscle*, calculated	3.31
Intercostal muscle, measured	3.30
Bone**, calculated	3.19
Rib bone, measured	3.02

Composition in per cent:
* 10.2 H, 12.3 C, 3.5 N, 72.9 O, 0.08 Na, 0.2 Mg, 0.2 P, 0.5 S, 0.3 K.
** 6.4 H, 27.8 C, 2.7 N, 41.0 O, 0.2 Mg, 7.0 P, 0.2 S, 14.7 Ca.

influence on the dose distribution when the heterogeneities consist of objects with small cross-sectional areas, for example between 0.5 cm × 1.5 cm and 1 cm × 2 cm. Ribs and costal cartilage constitute structures of small cross-sectional areas. Accordingly, scatter effects should be considered. Two adjacent ribs will for instance scatter electrons into the interstice in between, thus causing superimposed energy deposition. This will result in alternating high and low dose regions in the chest wall. BREITLING (1963) has demonstrated this effect in a model experiment using 16.2 MeV electrons. The effect would be still more marked for lower energies as the scatter angle is strongly dependent on the electron energy. In the investigation of the absorbed dose distribution behind specimens of the chest wall by TLD measurements (RAGNHULT et coll. 1972) it was found that at the electron energy of 10 MeV the variation was ±10 per cent and at 13 MeV it was reduced to ±5 per cent. It was suggested that the great dispersion of the dose could be explained by the influence of scattering effects occurring when the high-energy electrons interacted with the different components of the multi-structured chest wall. In order to find experimental evidence for the magnitude of the effect, the electron densities in the different tissue materials were determined. After correction of an error in the previous report (unfortunately the electron content for costal cartilage was over-estimated in the report of 1972, instead of 3.30×10^{23} it should be 3.15×10^{23} g^{-1}), it was found that the greatest difference in mean values of electron densities for various types of tissue existed between rib bone and fatty tissue and that it could be expected to exceed 8 but not 16 per cent. The most marked discontinuity existed at the interfaces between rib bone and intercostal soft tissue of muscles and interlaced fat. The results given in Table 5 are plotted in Fig. 5 and normalized to intercostal soft tissue. In the same diagram the relative densities are also plotted. It was found that the mean densities of the different types of tissue varied by 17 per cent, while the variation in mean elec-

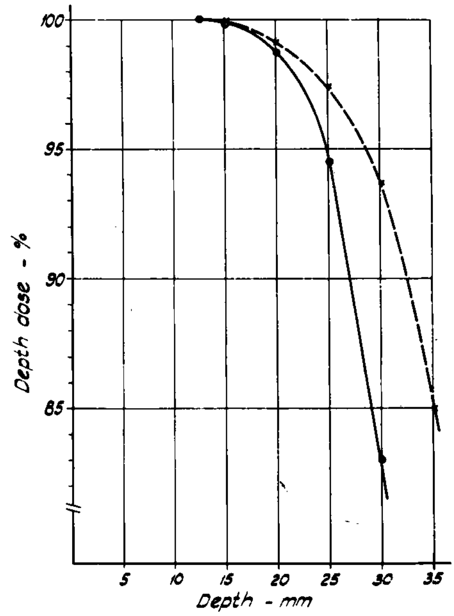

Fig. 6. Central axis depth dose curves for 10 (——) and 13 (– – –) MeV electrons in the depth of interest.

tron densities amounted to only 7 per cent. If the maximum deviations were taken into account, however, the greatest difference in density amounted to 30 per cent and the corresponding difference in electron density to 18 per cent, values which in fact partly explain the dispersion of absorbed dose found in the previous report.

The complex chemical composition of sternum, ribs and costal cartilage makes it difficult to calculate the electron content for these compounds. ICRU (1972) assumes for muscle tissue and compact bone the elementary composition given in Table 6. The electron content in these compounds were calculated and compared with the measured values in Table 5 for intercostal muscle tissue and rib bone. The results appear in Table 6. The values for muscle tissue agree closely, while the electron content of rib is 5.5 per cent less than that of compact bone. This is reasonable because only a thin shell of compact bone surrounds the spongy parts of rib.

Clinical considerations. In the irradiation of the lymph glands along the internal thoracic vessels the target volume includes intercostal soft tissue, rib bone, costal cartilage and the sternum. Internal mammary lymph nodes may be covered in part by costal cartilage especially in the first and second intercostal spaces (DAHL-IVERSEN 1951). URBAN (1959) reported the incidence of internal mammary lymph nodes to be 91 per cent at the first intercostal space, 89 per cent at the second, 75 per cent at the third, 53 per cent at the fourth and 13 per cent at the fifth.

Within and adjacent to the target volume there are organs and tissues in which high doses of radiation may produce deleterious changes. During left-sided irradiation the anterior part of the pericardium, parts of the anterior wall of the right ven-

Table 7

Reduction of relative depth doses in regions beyond heterogeneities. Calculations are made for a depth of 28 mm using formula (7). The thicknesses and relative electron densities were maximum values. (The value for sternum of specimen 1 was excluded)

Heterogeneity	Relative electron density	Maximal thickness mm	Reduction of depth dose (per cent)	
			10 MeV	13 MeV
Rib bone	1.17	6	2.6	0.8
Costal cartilage	1.06	10	1.6	0.4
Sternum	1.05	14	1.9	0.5

tricle and the left coronary artery will fall within or close to the target volume. The situation is somewhat more favourable in right-sided irradiation. In both cases the lungs will be close to the margin of the target volume. In view of the proximity of these critical organs and the superficial position of the lymph glands, the use of electron radiation with a very limited depth of penetration is advisable.

In clinical practice a limited overdosage in small regions is considered to be of little significance for the radiation effect. Thus, the high dose regions caused by scattered electrons may be neglected. It is, however, essential for successful therapy that no point within the target volume receives a lower absorbed dose than prescribed and, consequently, the reduction of absorbed dose beneath heterogeneities should be considered in treatment planning.

The thickness of the chest wall, in the parasternal region after Halsted's operation, has, in the present investigation been determined to be less than or equal to 30 mm and the mean depth of the lymph glands 20 mm with a maximum deviation of ± 8 mm. Fig. 6 gives the relevant parts of the central depth dose curves for 10 and 13 MeV electron radiation from a BBC betatron (Asklepitron 35) measured in a polystyrene phantom. The energies were determined as recommended by the Nordic Association of Clinical Physics (1972). Polystyrene has a density of 1.04 g cm^{-3} and an electron density of 0.338 10^{24} cm^{-3}, values which are very similar to the corresponding ones for soft tissue.

Considering a lymph gland at the depth of d mm situated beneath a heterogeneity with the thickness t mm, an effective depth DE could be calculated from the formula

$$DE = d + (r - 1) \times t \qquad (7)$$

where r is the ratio of electron densities for heterogeneity and intercostal soft tissue. This method of calculation does not allow for the effects of scattered electrons and should be used for estimation of the absorbed dose at a depth beyond the heterogeneity (Boone et coll. 1969).

The expression (7) and the central depth dose curves in Fig. 6 were used for the determination of the reduction of relative depth doses given in Table 7. Here are

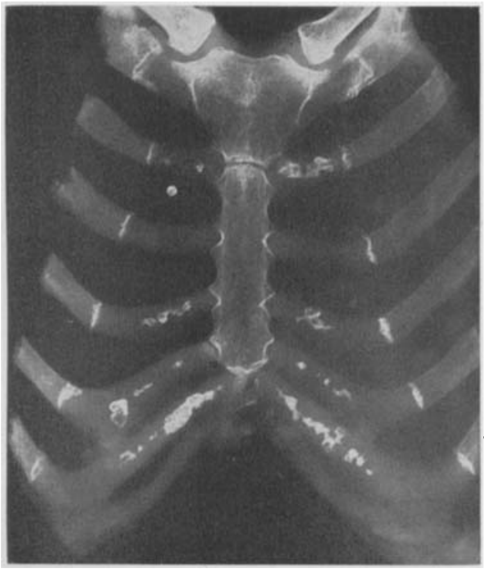

Fig. 7. Tissue block of the anterior thoracic wall.

considered the most difficult cases found in this investigation, viz. glands at the depth of 28 mm, positioned beyond heterogeneities of maximal thickness and maximal electron densities. The effective depths DE differ from the real depth by 1 mm for rib bone and less in the other cases. The reduction of relative depth dose is maximally 2.6 per cent, which occurs for rib bone. This reduction is too small to need consideration in clinical practice and 10 MeV electrons can thus be used in treatment of the mammary glands, though a somewhat higher energy should have the advantage of reduced scattering effects. For energies higher than 13 MeV, however, parts of the lung tissue and the myocardium would receive more than 90 per cent relative absorbed dose. Thus, 13 MeV was considered as the highest recommendable energy in the cases where underlying critical tissue was to be spared.

Conclusions. The electron densities of different types of tissue in 8 specimens of the anterior chest wall of human beings were determined. The mean electron densities of the different types of tissue varied by 7 per cent, while the maximum deviation was 18 per cent. Using the determined values it was estimated that underdosage beneath heterogeneities could be limited to 2.6 per cent of the relative depth dose if electron energies not lower than 10 MeV were used. Considering critical tissues underlying the target volume, 13 MeV was recommended as an upper limit of energy. Thus, it was concluded that electron radiation in the energy range of 10 to 13 MeV could be used for treating the internal mammary glands.

Attenuation of 10 and 13 MeV electrons in the anterior chest wall

Attenuation of high-energy electron radiation in human tissue has been investigated by several authors (see LAUGHLIN 1969). The attenuation of high-energy elec-

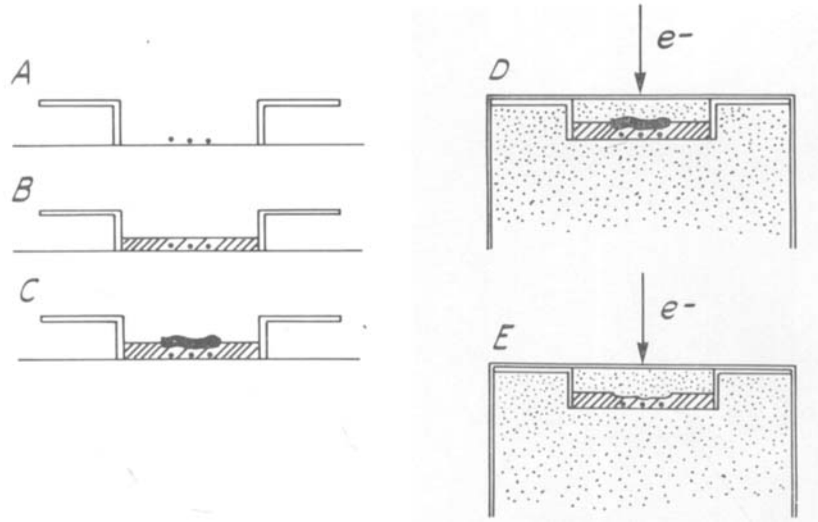

Fig. 8. Schematic principle of the experimental method. A. Catheters and perspex frame placed horizontally on a level surface. B. Molten paraffin wax covers the catheters. C. The specimen pressed down over the catheters in the paraffin. D. Perspex frame, with specimen and catheters fixed in the set paraffin, lowered vertically into a water phantom and fixed to the front wall of the phantom. Before irradiation the catheters are filled with probes containing TLD dosimeters. E. Repeated irradiation with the specimen removed and new probes introduced into the catheters.

trons in bone and water was determined by HATTORI & KITABATAKE (1968), who found that the difference was negligible for the energy range 16 to 31 MeV. BOONE et coll. (1967, 1969) estimated the attenuation of electrons in the anterior chest wall of dogs using energies from 6 to 15 MeV. They concluded that the distribution of absorbed dose was significantly perturbed when electrons with energies between 6 and 9 MeV were used but that the reduction of absorbed dose beneath the inner aspect of the chest wall between 12 and 15 MeV was negligible.

To determine the reduction of absorbed dose behind fresh specimens of ribs, costal cartilages and sternum (Fig. 7) an experimental technique was developed enabling dosimeters to be placed immediately under the specimens in regions in which low absorbed dose was to be expected and little influence of electrons scattered from the surroundings.

Methods

Measurements of absorbed dose were performed by means of thermoluminescent dosimetry. Small LiF-teflon dosimeters (cylinders, 6 mm × 1 mm) were used, inserted into teflon tubes (wall thickness 0.25 mm). The instrument and the measuring technique used have been described previously (LINDSKOUG et coll. 1967, JOHANSSON et coll. 1969).

Two tissue blocks of the anterior thoracic wall were used. After removal of the soft tissues from the surfaces of the specimens, the densities of the specimens were determined.

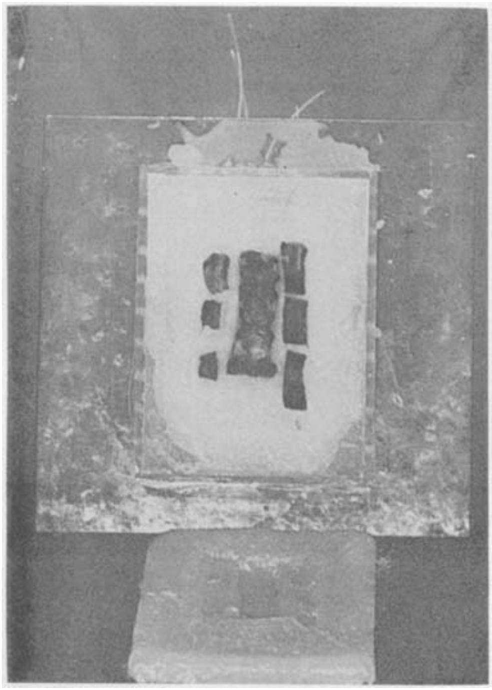

Fig. 9. Specimen mounted in paraffin surounded by a perspex frame. Catheters emerging behind the upper edge of the perspex frame.

Catheters made of teflon were fixed in a perspex frame and molten paraffin wax was poured over them to a thickness of approximately 15 mm. The experimental set-up is schematically illustrated in Fig. 8. Specimens of the dissected tissue block were gently pressed into the paraffin and positioned right over the catheters (Fig. 9). The dosimeters were surrounded by paraffin ($C_{16}H_{34}$), which has an electron density about 4 per cent lower than that of water. Thus, electron back and side-scatter contribution from the paraffin to the dosimeters should be very small, compared with the corresponding scatter contribution from intercostal soft tissue which has an electron density 1.024 times higher than water. The frame with the paraffin sheet, specimens and catheters was placed vertically in a water phantom (Fig. 10) and fixed to the 5 mm thick polystyrene wall. Probes containing LiF dosimeters were introduced into the catheters and irradiation was performed by means of a BBC betatron (Asklepitron 35). The absorbed dose to water was always 100 rad at the depth of the dose maximum. The specimens were then carefully removed from the paraffin sheet without changing the position of the perspex frame and irradiation repeated using new probes in the catheters. The geometry was thus unchanged but water was substituted for the tissue block. The depths of the structures and dosimeters were as follows:

From front surface of phantom to front surface of specimen 6–18 mm, from back surface of specimen to point of measurement 2–5 mm, and total depth of measurement 20–26 mm.

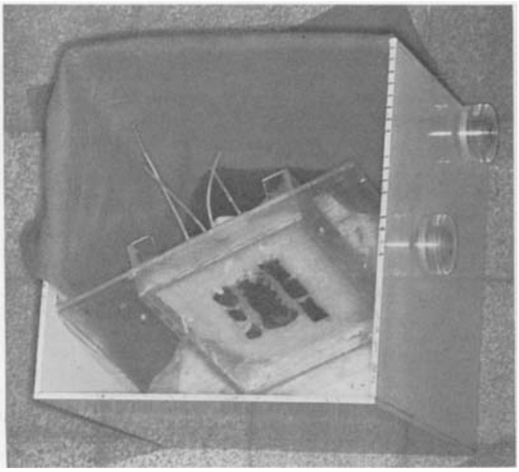

Fig. 10

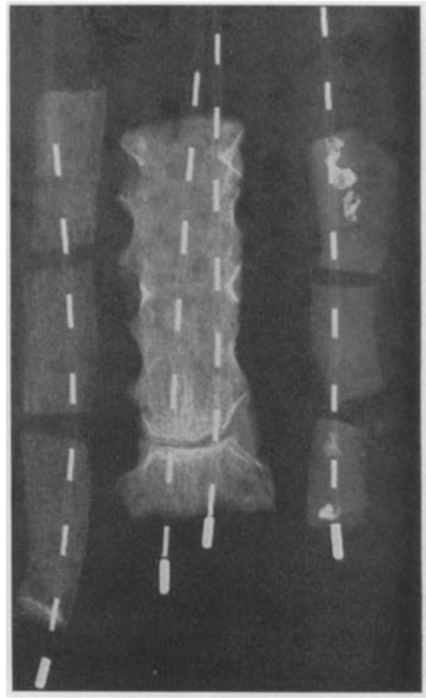

Fig. 11

Fig. 10. Perspex frame with specimen and catheters in an unfilled water phantom.

Fig. 11. Mounted specimen. Sternum and manubrium, ribs and costal cartilage. Catheters filled with indicator probes.

The paraffin sheet with various specimens and probes containing indicators of copper inserted into the catheters appear in Fig. 11.

Result

The results of the determinations are given in Table 8. The three columns to the left give information about the type of specimen and the number of dosimeters used, the mean dimension of the specimen in the direction of radiation, the mean density of the different specimens and their respective standard deviations. The dimensions of the specimens are given for the sections lying directly in front of each dosimeter. The next three columns represent the absorbed doses and the relative absorbed doses determined for an electron energy of 10 MeV. The three columns to the far right show the corresponding results for 13 MeV electrons. The relative absorbed dose is given for the heterogeneous case (specimen) in percentage of the homogeneous case (water). The overall mean values for the different specimens appear in Table 9.

It is evident that the reduction of absorbed dose for the energy of 10 MeV did not in any case exceed 3 per cent. For the energy of 13 MeV it seems doubtful whether reduction of absorbed dose is significant.

The tissue blocks used were taken from bodies of rather high age, with calcium

Table 8

Results for two tissue blocks (A and B) irradiated with 10 and 13 MeV electrons. Relative absorbed dose calculated for the heterogeneous case (specimens) in percentage of the homogeneous case (water). Number of measurement points (within brackets) and standard deviations (SD) are given on the second lines

Material	Dimension in the direction of radiation (mm)	Density g cm^{-3}	10 MeV Absorbed dose		Spec./water Rel. dose (per cent)	13 MeV Absorbed dose		Spec./water Rel. dose (per cent)
			Water (rad)	Specimen (rad)		Water (rad)	Specimen (rad)	
A								
Rib bone	3.7	1.22	98.3	95.8	97.5	108.5	105.5	97.2
SD (6)	0.8		1.0	2.0	1.7	1.0	0.5	1.0
Sternum	10.9	1.13	98.8	95.8	97.0	106.0	108.9	102.9
SD (10)	2.1		4.5	4.7	2.5	5.4	4.7	4.5
Costal cartilage	5.0	1.10	97.2	95.8	98.5	100.6	103.6	103.0
SD (5)	0.8		2.6	4.6	2.4	3.3	3.8	2.6
B								
Rib bone	4.8	1.13	72.8	73.7	101.1	88.8	91.7	103.2
SD (6)	0.8		2.8	3.8	2.4	1.7	3.0	1.9
Sternum	10.5	1.08	80.4	79.8	99.3	91.7	89.4	97.6
SD (12)	1.2		4.1	4.3	2.6	2.8	1.8	1.9
Costal cartilage	8.6	1.19	66.2	65.6	99.1	86.0	84.0	98.0
SD (5)	1.1		1.8	1.8	2.9	5.5	0.7	5.8

salts already deposited in the cartilage matrix. Fig. 7 might give the impression that the calcified areas constitute important heterogeneities inside the costal cartilage. The film was, however, exposed with 40 kVp, which is a quality where the attenuation of photons is strongly dependent upon the atomic number (Z) of the irradiated material. Thus the calcified areas appear with high contrast in the image. The attenuation of electrons will, however, mainly depend upon electron density of the material but a significant dose reduction should still be expected beneath a calcified area. The dosimeters are too large, however, to allow detailed determination of the dose distribution in the regions beneath these small calcium deposits.

Discussion

Measurements in vivo will always be influenced by variations in field flatness. With the present experimental set-up variations in field flatness will be the same with and without specimen as they are irradiated with short intervals.

Table 9

Mean values for the two tissue blocks (A + B), and overall mean values

Material	Dimension in the direction of radiation (mm)	Density g cm^{-3}	10 MeV Absorbed dose Water (rad)	10 MeV Absorbed dose Specimen (rad)	Spec./water Rel. dose (per cent)	13 MeV Absorbed dose Water (rad)	13 MeV Absorbed dose Specimen (rad)	Spec./water Rel. dose (per cent)
Rib bone	4.3	1.19	86	85	99.3	99	99	100.2
SD (12)	1.0		13	12	2.7	10	8	3.4
Sternum	10.7	1.11	89	87	98.2	98	98	100.0
SD (22)	1.6		10	9	2.8	8	10	4.2
Costal cartilage	6.9	1.08	82	81	98.8	93	94	100.5
SD (10)	2.0		16	16	2.5	9	11	5.0
Overall mean values	8.1	1.13	86	85	98.7	97	97	100.2
SD (44)	3.2		13	12	2.7	9	10	4.1

It may be concluded that the attenuation of electron radiation in the energy range 10 to 13 MeV in rib, costal cartilage and sternum does not differ significantly from that in soft tissue. The highest reduction of absorbed dose compared with the reduction in water was found to be 3 per cent which was valid for ribs. This was within the limits of precision for the TLD measurements (JOHANSSON et coll.). The results confirm the conclusion that electron radiation in the energy range of 10 to 13 MeV can be utilized for irradiation of internal mammary lymph nodes without risk of underdosage.

Acknowledgements

The authors are particularly indebted to Prof. Holger Sköldborn for valuable discussion and encouragement throughout the investigation. For constructive criticism we thank Prof. C. Carlsson. This investigation has been partly financed by funds made available by the Swedish Cancer Society and partly by funds provided by the Faculty of Medicine, University of Gothenburg, Sweden.

SUMMARY

The density (g cm^{-3}) and electron density (cm^{-3}) of material from the anterior chest wall was determined. On the average, the difference in density between rib bone and intercostal soft tissue amounted to 17 per cent, while the difference in electron density was 7 per cent. The attenuation of high-energy electrons in specimens of rib bone, costal cartilage and sternum was determined by an experimental technique, using dosimeters of TLD material. The results of determinations of attenuation of 10 and 13 MeV electrons in fresh specimens are presented. It is concluded that electron radiation in the energy range of 10 to 13 MeV can be utilized for irradiation of lymph glands along the internal thoracic vessels without risk of underdosage.

ZUSAMMENFASSUNG

Die Dichte (g cm^{-3}) und Elektronendichte (cm^{-3}) der Gewebe der vorderen Brustwand wurden bestimmt. Im Durchschnitt betrug die Differenz in der Dichte zwischen dem Rippenknochen und dem intercostalen Weichteilgewebe 17 Prozent, während die Differenz in der Elektronendichte 7 Prozent betrug. Die Abnahme der hochenergetischen Elektronen in Proben von Rippenknochen, Rippenknorpel und Brustbein wurde durch einen experimentellen Test unter Verwendung von Dosimetern aus TLD Material bestimmt. Die Ergebnisse der Bestimmungen über die Abnahme von 10 und 13 MeV Elektronen in frischen Geweben werden gegeben. Die Verfasser schliessen daraus, dass die Elektronenbestrahlung im Energiebereich zwischen 10 und 13 MeV zur Bestrahlung der Lymphknoten längs der inneren Thoraxgefässe ohne Risiko einer Unterdosierung verwendet werden kann.

RÉSUMÉ

Les auteurs ont mesuré la densité (g cm^{-3}) et la densité électronique (cm^{-3}) de tissus de la paroi thoracique antérieure. En moyenne la différence de densité entre l'os costal et les tissus mous inter-costaux est de 17% alors que la différence de densité électronique est de 7%. L'atténuation des électrons de haute énergie dans des fragments d'os costal, de cartilage costal et de sternum a été déterminée par un test expérimental utilisant des dosimètres en matériaux pour TLD (matériaux pour dosimétrie par thermoluminescence). Les auteurs présentent les résultats des mesures d'atténuation d'électrons de 10 et de 13 MeV pour des fragments anatomiques frais. Ils concluent que le rayonnement électronique dans le domaine d'énergie entre 10 et 13 MeV peut être utilisé pour l'irradiation de ganglions lymphatiques le long des vaisseaux thoraciques internes sans risque de sous-dosage.

REFERENCES

BOONE M. L. M., ALMOND P. R. and WRIGHT A. E.: High-energy electron dose perturbations in regions of tissue heterogeneity. *In*: High-energy radiation therapy dosimetry. Ann. N.Y. Acad. Sci. 161 (1969), 214.

— JARDINE J. H., WRIGHT A. E. and DU V. TAPLEY N.: High-energy electron dose perturbations in regions of tissue heterogeneity. Radiology 88 (1967), 1136.

BREITLING G. und VOGEL K-H.: Dosisverteilung bei der Bestrahlung inhomogener Medien mit schnellen Elektronen. Strahlentherapie 122 (1963), 321.

BRENNER M., KARJALAINEN. P., RYTILLÄ A. and JUNGAR H.: The effect of inhomogeneities on dose distributions of high-energy electrons. *In*: High-energy radiation therapy dosimetry. Ann. N.Y. Acad. Sci. 161 (1969), 233.

DAHL-IVERSEN E.: Carcinoma of the breast. Transactions of the twenty-fifth meeting of the Northern Surgical Association in Copenhagen (1951), 150. Ejnar Munksgaard, Köpenhamn 1951.

DAHLER A., BAKER A. S. and LAUGHLIN J. S.: Comprehensive electron-beam treatment planning. *In*: High-energy radiation therapy dosimetry. Ann. N.Y. Acad. Sci. 161 (1969), 198.

DEBOIS J. M. and DE ROO M.: Experimental demonstration of the influence of bone on dose distribution in radiotherapy. Radiology 92 (1969), 1.

DUTREIX A.: Correction of single-field distributions to allow for tissue inhomogeneity. IAEA technical reports series No 57. Computer calculation of dose distributions in radiotherapy (1966), 74.

HATTORI H. and KITABATAKE T.: Influence of bone tissue upon dose distribution in high-energy electron beam therapy. Tohoku J. exp. Med. 95 (1968), 351.

ICRU Report 21: Radiation dosimetry: Electrons with initial energies between 1 and 50 MeV. International commission on radiation units and measurements, Washington USA, 1972.

JOHANSSON J. M., LINDSKOUG B. and NYSTRÖM C.: Pelvic dosimetry during radiotherapy of carcinoma of the cervix uteri. Acta radiol. Ther. Phys. Biol. 8 (1969), 360.

KARJALAINEN P., BRENNER M. and RYTILLÄ A.: Effect of anatomical irregularities on the dose in electron beam therapy. Acta radiol. Ther. Phys. Biol. 7 (1968), 129.

LAUGHLIN J. S., Editor.: High-energy radiation therapy dosimetry. Ann. N.Y. Acad. Sci. 161, (1969), 1.

LINDSKOUG B., JOHANSSON M., KARLSSON R. and KELLGREN R.: Measuring device for thermoluminescence dosimetry. J. sci. Instrum. 44 (1967), 939.

Nordic Association of Clinical Physics: Procedures in radiation therapy dosimetry with 5 to 50 MeV electrons and roentgen and gamma rays with maximum photon energies between 1 and 50 MeV. Acta radiol. Ther, Phys. Biol. 11 (1972), 603.

POHLIT W.: Calculated and measured dose distribution in inhomogeneous materials and in patients. *In*: High-energy radiation therapy dosimetry. Ann. N.Y. Acad. Sci. 161 (1969), 189.

RAGNHULT I., LINDSKOUG B. and HULTBORN A.: Dosimetric investigation of postoperative irradiation of regional lymph nodes in mammary carcinoma. Acta radiol. (1972) Suppl. 313, p. 135.

ROOS B., ROSENGREN B. and SKÖLDBORN H.: Determination of bone mineral content in lumbar vertebrae by a double gamma-ray technique. Proceedings of bone measurement conference. United States Atomic Energy Commission Division of Technical Information, Chicago, Illinois (1970), 243.

TRÜBESTEIN H.: Die "absorbierte Dosis" im Gewebe für Röntgenstrahlen von 10 keV bis 1 MeV und die Gewebsdichte. Strahlentherapie 111 (1960), 122.

URBAN J. A.: Clinical experience and results of excision of internal mammary lymph node chain in primary operable breast cancer. Cancer 12 (1959), 14.